J. Appl. Comput. Mech., 8(3) (2022) 940-948
DOI: 10.22055/JACM.2020.35060.2550
ISSN: 2383-4536
jacm.scu.ac.ir

Shahid Chamran University of Ahvaz

Journal of Applied and Computational Mechanics

Research Paper

Combined Impacts of Fin Surface Inclination and Magnetohydrodynamics on the Thermal Performance of a Convective-Radiative Porous Fin

Gbeminiyi M. Sobamowo

Department of Mechanical Engineering, University of Lagos, Nigeria

Received September 16 2020; Revised November 19 2020; Accepted for publication November 19 2020.
Corresponding author: G.M. Sobamowo (gsobamowo@unilag.edu.ng ; mikegbeminiyi@gmail.com)

Abstract. In this work, the combined impacts of magnetohydrodynamics and fin surface inclination on thermal performance of convective-radiative porous fin with temperature-invariant thermal conductivity is numerically study using finite difference method. Parametric studies reveal that as the inclination of fin, convective, radiative, magnetic and porous parameters increase, the adimensional fin temperature decreases which leads to an increase in the heat transfer rate through the fin and the thermal efficiency of the porous fin. It is established that the porous fin is more efficient and effective for low values of convective, inclination angle, radiative, magnetic and porous parameters. The thermal performance ratio of the fin increases with the porosity parameter.

Keywords: Convective-radiative fin; Fin surface inclination; Magnetohydrodynamics; Thermal analysis; Thermal Performance.

1. Introduction

The applications of fins as passive devices for thermal management of electronics and thermal systems have grown exponentially. Although, solid fins have been applied as passive devices for cooling and thermal control of thermal and electronics equipment, further heat transfer enhancement has been achieved through the use of porous fins. The importance of such fins in various thermal and electronic equipment aroused various studies. In these studies, Kiwan and Al-Nimir [1] pointed out use of fins with pores for thermal augumentation of the extended surfaces. Gong et al. [2] illustrated the used of porous and solid compound fins for heat sink in micro-channel. Ali et al. [3] experimentally investigated the effects of heat sink fin shapes and phase change materials on the thermal cooling of electronics. Saedodin [4] presented numerical analysis of temperature distribution in natural convection fins with pores while Sobamowo et al. [5] applied Galerkin method of weighted residual for the analysis of the temperature distribution in the natural convection porous fins. Oguntala et al. [6] explored the impact of particle deposition on the thermal bahaviour of heat sink porous fins with convective and radiative heat transfer. Mosayebidorcheh et al. [7] investigated the transient response of fins with different shapes and variable thermal properties and internal heat generation. Kim and Mudawar [8] also examined the shapes effects on heat diffusion through an heat sink. Moradi et al.[9] adopted differential transformation method to analyze fins with triangular profiles and temperature-variant thermal conductivity. The influence of magnetic field on a convection-radiative rectangular porous fins with variable thermal conductivity was investigated by Oguntala et al. [10]. Wan et al. [11] experiementally studied the fluid flow and heat transfer in a miniature porous heat sink under high heat flux application while Naphon et al.[12] had earlier presented a numerical investigation of fluid flow and heat transfer in the mini-fin heat sink. Optimum design and thermal stability of an extended surface with variable thermal properties and internal heat generation was studied by Oguntala et al. [13] while Sobamowo [14] applied Galerkin's method of weighted residual to examine the thermal performance of rectangular fin with variable thermal properties and internal heat generation. Seyf and Feizbakhshi [15] submitted a computational study on the effects of nanofluid on the heat transfer capacity of micro-pin-fin heat sinks. Fazeli et al. [16] presented both experimental and numerical investigations of the effect of silica nanofluid on the heat transfer in a miniature heat sink. Additionally, Oguntala et al. [17, 18] and Sobamowo et al. [19] displayed the efficacy of some new analytical and numerical methods in the thermal analysis of the porous fins.

In the applications of fin for the heat transfer enhancement, it is established that the thermal conductivities of the materials for fins are temperature-dependent. Therefore, the effects of the temperature-dependent thermal properties on the fin performance have been taken into consideration in previous studies. However, it has been established that when there is small temperature variation exists between the base and the tip of the fin, the thermal conductivity of the fin can be taken constant. Also, it has been shown that the thermal conductivity of palladium is constant at a relatively low temperature (-100°C – 227°C). Therefore, thermal analysis of fins with temperature-invariant thermal conductivity has applications in such situations. In some

Published online: April 03 2021

other studies, the effects of inclination of fins on the thermal performance of the extended surfaces have been studied by Sobamowo et al. [20], Gireesha and Sowmya [21] and Jasim and Söylemez [22] and Oguntala et al. [23]. However, to the best of the author's knowledge, a study of combined effects of combined impacts of magnetohydrodynamics and inclination of fin on thermal performance of convective-radiative porous fin with temperature-invariant thermal conductivity is numerically study using finite difference method. The effects of the other parameters of the thermal model parameters on the heat transfer behaviour of the extended surface are also investigated

2. Problem formulation

Consider a longitudinal rectangular fin with pores having convective and radiative heat transfer as shown in Fig. 1. The fin is inclined at an angle γ to the horizontal axis (x-axis) as shown in Fig. 2. In order to derive the thermal model of the porous fin, it is assumed that the porous medium is isotropic, homogeneous and it is saturated with single-phase fluid. The physical and thermal properties of the fin and the surrounding fluid surface are constant. The temperature varies in the fin is only along the length of the fin as shown in the Fig. 1. and there is a perfect contact between the fin base and the prime surface.

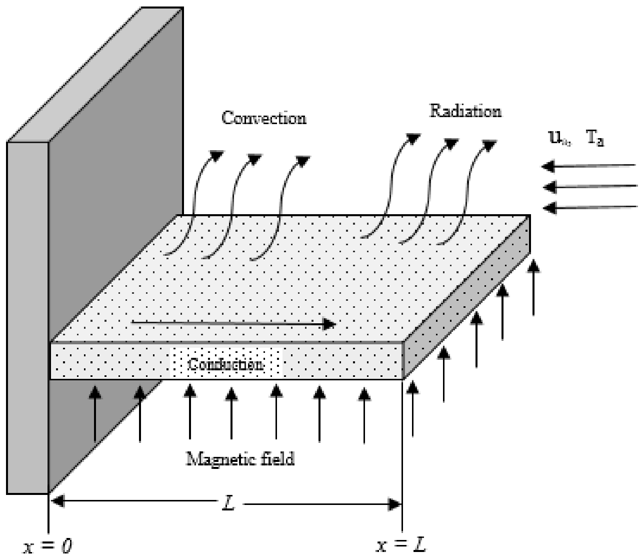

Fig. 1. Schematic configuration of the convective-radiative longitudinal porous fin subjected to magnetic field

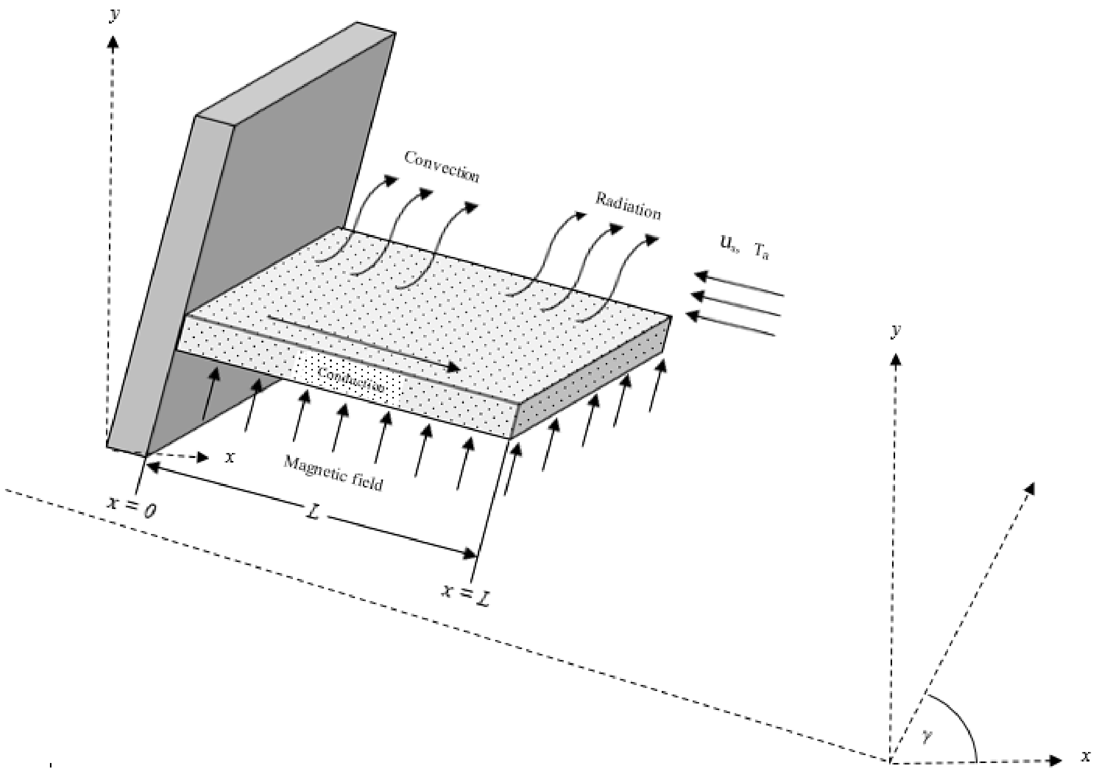

Fig. 2. Schematic configuration of convective-radiative longitudinal porous fin inclined at an angle γ to the horizontal axis

From the assumptions and with the aid of Darcy's model, the energy balance is:

$$q_x - \left(q_x + \frac{\delta q}{\delta x}dx\right) = \dot{m}c_p(T - T_a) + hP(1-\varepsilon)(T - T_a)dx + \sigma\varepsilon P(T^4 - T_a^4)dx + \frac{J_c \times J_c}{\sigma}dx \tag{1}$$

The fluid flows through the pores at the rate of mass flow given as

$$\dot{m} = \rho u(x)Wdx \tag{2}$$

Also, the fluid velocity is given as

$$u(x) = \frac{gK\beta_R(T - T_a)\sin(\gamma)}{\nu} \tag{3}$$

Then, Eq. (1) becomes

$$q_x - \left(q_x + \frac{\delta q}{\delta x}dx\right) = \frac{\rho c_p gK\beta_p}{\upsilon}(T - T_a)^2\sin(\gamma)dx + hP(1-\varepsilon)(T - T_a)dx + \sigma\varepsilon P(T^4 - T_a^4)dx + \frac{J_c \times J_c}{\sigma}dx \tag{4}$$

As $dx \rightarrow 0$, Eq. (4) reduces

$$-\frac{dq_x}{dx} = \frac{\rho c_p gK\beta_p}{\upsilon}(T - T_a)^2\sin(\gamma) + hP(1-\varepsilon)(T - T_a) + \sigma\varepsilon P(T^4 - T_a^4) + \frac{J_c \times J_c}{\sigma} \tag{5}$$

Applying Fourier's law for the heat conduction in the solid, one has

$$q_C = -k_{eff}A_{cr}\frac{dT}{dx} \tag{6}$$

where the effective thermal conductivity of the fin is given as

$$k_{eff} = \phi k_f + (1-\phi)k_s \tag{7}$$

According to Roseland diffusion approximation, the radiative heat transfer rate can be written as

$$q_R = -\frac{4\sigma A_{cr}}{3\beta_R}\frac{dT^4}{dx} \tag{8}$$

From Eqs. (6) and (8), the total rate of heat transfer is given by

$$q_T = -k_{eff}A_{cr}\frac{dT}{dx} - \frac{4\sigma A_{cr}}{3\beta_R}\frac{dT^4}{dx} \tag{9}$$

Substitution of Eq. (9) into Eq. (6) leads to

$$\frac{d}{dx}\left(k_{eff}A_{cr}\frac{dT}{dx} + \frac{4\sigma A_{cr}}{3\beta_R}\frac{dT^4}{dx}\right) = \frac{\rho c_p gK\beta_p}{\upsilon}(T - T_a)^2\sin(\gamma) + hP(1-\varepsilon)(T - T_a) + \sigma\varepsilon P(T^4 - T_a^4) + \frac{J_c \times J_c}{\sigma} \tag{10}$$

Expansion of the first term in Eq. (10), provides the governing equation for the required heat transfer

$$\frac{d^2T}{dx^2} + \frac{4\sigma}{3k_{eff}\beta_R}\frac{d}{dx}\left(\frac{dT^4}{dx}\right) - \frac{\rho c_p gK\beta_p}{t\upsilon k_{eff}}(T - T_a)^2\sin(\gamma) - \frac{h(1-\varepsilon)(T - T_a)}{k_{eff}t} - \frac{\sigma\varepsilon}{k_{eff}t}(T^4 - T_a^4) - \frac{J_c \times J_c}{\sigma} = 0 \tag{11}$$

The boundary conditions are

$$\begin{gathered} x = 0,\ \frac{dT}{dx} = 0, \\ x = L,\ T = T_b \end{gathered} \tag{12}$$

But

$$\frac{J_c \times J_c}{\sigma} = \sigma B_o^2 u^2 \tag{13}$$

After substitution of Eq. (13) into Eq. (11), we have

$$\frac{d^2T}{dx^2} + \frac{4\sigma}{3k_{eff}\beta_R}\frac{d}{dx}\left(\frac{dT^4}{dx}\right) - \frac{\rho c_p gK\beta_p}{t\upsilon k_{eff}}(T - T_a)^2\sin(\gamma) - \frac{h(1-\varepsilon)(T - T_a)}{k_{eff}t} - \frac{\sigma\varepsilon}{k_{eff}t}(T^4 - T_a^4) - \frac{\sigma B_o^2 u^2}{k_{eff}A_{cr}}(T - T_a) = 0 \tag{14}$$

The term T^4 can be expressed as a linear function of temperature as

$$T^4 = T_a^4 + 4T_a^3(T - T_a) + 6T_a^2(T - T_a)^2 + \ldots \approx 4T_a^3T - 3T_a^4 \tag{15}$$

Substitution of Eq. (13) into Eq. (11), results in

$$\frac{d^2T}{dx^2} + \frac{16\sigma}{3k_{eff}\beta_R}\frac{d^2T}{dx^2} - \frac{\rho c_p gK\beta_p}{t\upsilon k_{eff}}(T - T_a)^2\sin(\gamma) - \frac{h(1-\varepsilon)(T - T_a)}{k_{eff}t} - \frac{4\sigma\varepsilon T_a^3}{k_{eff}t}(T - T_a) - \frac{\sigma B_o^2 u^2}{k_{eff}A_{cr}}(T - T_a) = 0 \tag{16}$$

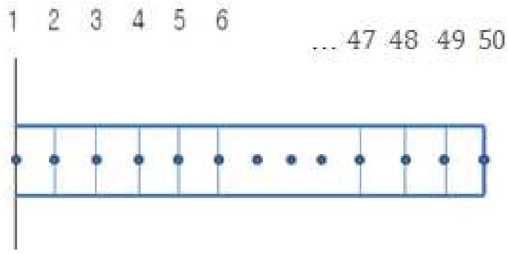

Fig. 3. Nodal representation for finite difference method

Applying the following nondimensional parameters in Eq. (15) to Eq. (14),

$$X=\frac{x}{L},\ \theta=\frac{T-T_a}{T_b-T_a},\ S_h=\frac{gK\beta_R(T_b-T_\infty)L}{\alpha\nu k_r},\ N_C=\frac{hL}{k_{eff}t},\ Ha=\frac{\sigma B_o^2u^2b}{k_{eff}A_b},\ Rd=\frac{4\sigma_{st}T_a^3}{3\beta_R k_{eff}},\ Nc=\frac{4\sigma_{st}LT_a^3}{tk_{eff}} \tag{17}$$

One arrives at the adimensional form of the governing Eq. (16) as presented in Eq. (18),

$$(1+4Rd)\frac{d^2\theta}{dX^2}-S_h\sin(\gamma)\theta^2-Nc(1-\varepsilon)\theta-Ha\theta=0 \tag{18}$$

and the nondimensional boundary conditions

$$\begin{gathered}X=0,\ \frac{d\theta}{dX}=0,\\ X=1,\ \theta=1\end{gathered} \tag{19}$$

3. Numerical Solution of the Thermal Model using Finite Difference Method

The numerical analysis of the nonlinear thermal model using finite difference method is presented in this section. The governing Eq. (18) and also, the boundary conditions in Eq. (19) are discretized as shown in Fig. 3, Eqs. (20) and (22):

$$(1+4Rd)\left(\frac{\theta_{i+1}-2\theta_i+\theta_{i-1}}{\triangle^2 X}\right)-S_h\sin(\gamma)\theta_i^2-M^2\theta_i-Nr\theta_i-Ha\theta_i=0 \tag{20}$$

From Eq. (20), the final algebraic form of the finite difference equation becomes

$$\theta_{i+1}-2\theta_i+\theta_{i-1}-\frac{S_h\sin(\gamma)(\triangle^2X)}{(1+4Rd)}\theta_i^2-\frac{M^2(\triangle^2X)}{(1+4Rd)}\theta_i-\frac{Nr(\triangle^2X)}{(1+4Rd)}\theta_i-\frac{Ha(\triangle^2X)}{(1+4Rd)}\theta_i=0 \tag{21}$$

The finite difference discretization of the boundary conditions is

$$\begin{gathered}i=1,\ \frac{\theta_2-\theta_0}{2\triangle X}=0\Rightarrow\theta_2=\theta_0\\ i=N,\ \theta_N=1\end{gathered} \tag{22}$$

From the above finite difference scheme in Eqs. (21) and (22), a set of 50 non-linear algebraic equations are developed. These systems of the non-linear equations are solved simultaneously with the aid of MATLAB using ***fsolve***.

4. Thermal Performance Indicator: Rate of Heat Transfer in the Porous Fin

The rate of heat transfer from the fin base is given by

$$q_b=kA_c\frac{dT}{dx} \tag{23}$$

Using the nondimensional parameters in Eq. (17), one arrives at the fin base dimensionless heat transfer rate as

$$Q_b=\frac{qL}{kA_c(T_b-T_\infty)}=\left[\frac{d\theta}{dX}\right]_{X=1} \tag{24}$$

The finite difference discretization of Eq. (24) is given

$$Q_b=\frac{qL}{kA_c(T_b-T_\infty)}=\left[\frac{\theta_{N+1}-\theta_N}{\triangle X}\right]_{X=1} \tag{25}$$

The fin rate of heat transfer per unit width is given as

$$Q_{b/w}=k(T_b-T_\infty)\left(\frac{t}{L}\right)\left[\frac{d\theta}{dX}\right]_{X=1} \tag{26}$$

Table 1. Comparison of results

X	HAM [24]	FDM (present work)	| FDM - HAM |
0.00	0.863499664	0.863499105	0.000000459
0.20	0.868776709	0.868776234	0.000000475
0.40	0.884696967	0.884696487	0.000000480
0.60	0.911531120	0.911530621	0.000000501
0.80	0.949741555	0.949741193	0.000000352
1.00	1.000000000	1.000000000	0.000000000

The finite difference discretization of Eq. (26) is given

$$Q_{b/w} = k(T_b - T_\infty)\left(\frac{t}{L}\right)\left[\frac{\theta_{N+1} - \theta_N}{\Delta X}\right]_{X=1} \tag{27}$$

The augmentation in the heat transfer achieved by the inclined porous fin can be established by comparing its rate of heat transfer to that of the solid fin, which is given as

$$\frac{q_b}{q_s} = \frac{k_{eff} A_b \left(dT/dx\right)_{x=0}}{hA_s(T_b - T_\infty)} \tag{28}$$

The denominator of Eq. (28) represents the maximum possible heat transfer rate by the solid fin. The nondimensional form of Eq. (28) is

$$\frac{q_b}{q_s} = \frac{A_r}{Nu}\left[\frac{d\theta}{dX}\right]_{X=1} \tag{29}$$

The finite difference discretization of Eq. (29) is given

$$\frac{q_b}{q_s} = \frac{A_r}{Nu}\left[\frac{\theta_{N+1} - \theta_N}{\Delta X}\right] \tag{30}$$

where the area ratio, $A_r = A_b / A_s$.

4. Results and Discussion

The numerical solutions are coded in MATLAB and the parametric and sensitivity analyses are carried out using the codes. Before the parametric and sensitivity analyses, the results of the developed solutions are verified with the results of homotopy analysis method (HAM) as presented by Amirkolaei *et al.* [24] shown in Table 1. The table show the verification of the results of the method used in this paper.

The impacts of inclination of fin, convective, radiative, magnetic and porous parameters on the adimensional temperature distribution, heat transfer at the fin base and thermal efficiency of the fin are presented in Figs. 4-8. It is shown in the figures that when the inclination of fin, convective, radiative, magnetic and porous parameters increase, the adimensional fin temperature decreases.

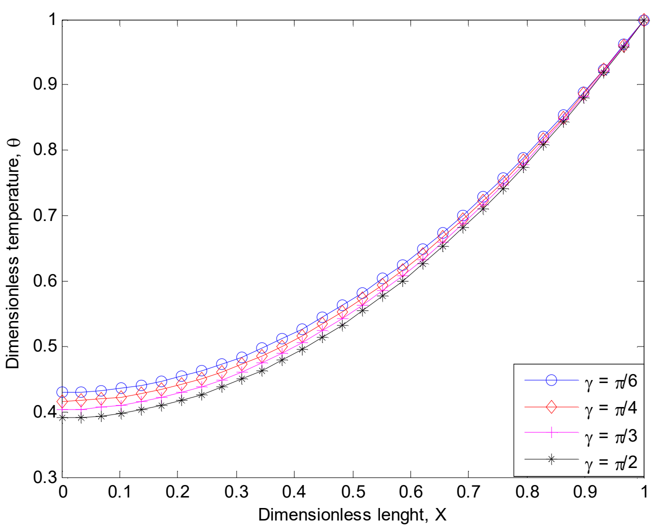

Fig. 4. Effects of inclination of fin on the nondimensional temperature distribution in the fin

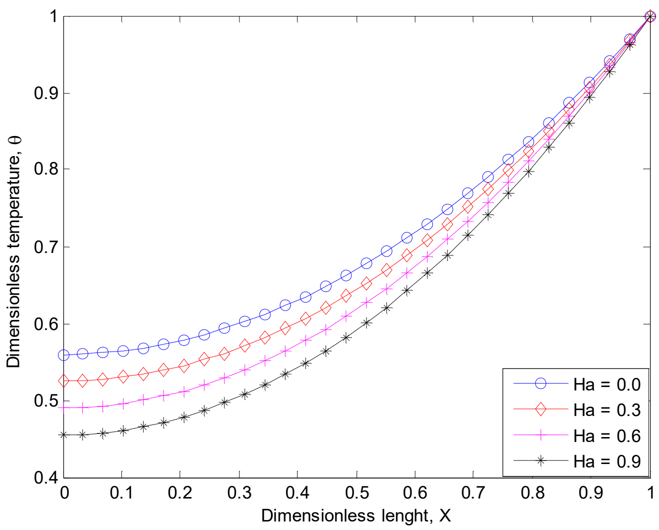

Fig. 5. Effects of Hartmann number on the nondimensional temperature distribution in the fin

The temperature drops along the fin increases as the inclination of fin, convective, radiative, magnetic and porous parameters increase. The physical implication of this is that the small values of convective and radiative parameter represent a relatively short and thick fins with poor thermal conductivity the while high values of the convective and radiative parameter correspond to a long fin or fin with low value of thermal conductivity. Since, the efficiency of the fin is maximum when the fin attains a uniform temperature which is the same as the temperature of the fin (T=T_b) and this can be achieved at low values of the inclination of fin, convective, radiative, magnetic and porous parameters, it can therefore be stated that very long fins with low thermal conductivity are to be avoided in practice. Also, the inclination of the fin and the magnetic effect should be kept as low as possible for improved thermal efficiency of the fin. The applications of the passive device can be seen in some thermal systems [25-27]

Figs. 4 shows the effect of inclination of fin on the dimensionless temperature distribution in the fin. The figure shows that as the inclination of fin increases (the vertical distance of the prime surface increases), the adimensional temperature distribution in the fin decreases (the fin thermal profile falls as shown in the figure). The reduction in the local temperature of the fin as the inclination of the fin increases is due to increase in the driving force for convection and buoyancy of the working fluid around the extended surface.

Fig. 5 illustrates the effect of Hartman number (magnetic field parameter) on the adimensional temperature distribution in the fin. The temperature in the fin decreases as the magnetic parameter increases. Increase in the magnetic parameter or Hartmann number causes increase in Lorentz force which provides resistive force that opposes motion of the working fluid around the fin and consequently, decreases the temperature of the fin.

Figs. 6 and 7 presents the influences of convective and radiative parameters on the dimensionless temperature distribution in the fin, respectively. The figures show that as the convective and radiative parameters increase, the adimensional local temperature in the fin decreases as the convective and radiative parameters. This is because, as the convective and radiative parameters increase, the effects of convective and radiative heat transfer on the fin surface increase, thereby, larger heat is taken away from the fin surface. As a consequent, surface temperature of the fin drops (the fin thermal profile falls) and the rate of heat transfer from the fin increases as the convective and radiative parameters increase. It should be noted that the low value of the convective and radiative parameters, Nc and Ra implies a relatively thick and short fin of very high thermal conductivity while a high value of the convective and radiative parameters indicates a relatively thin and long fin of a very low thermal conductivity. Therefore, the thermal efficiency of the fin is favoured at low values of convective and radiative parameters, i.e. a relatively thick and short fin with a high thermal conductivity.

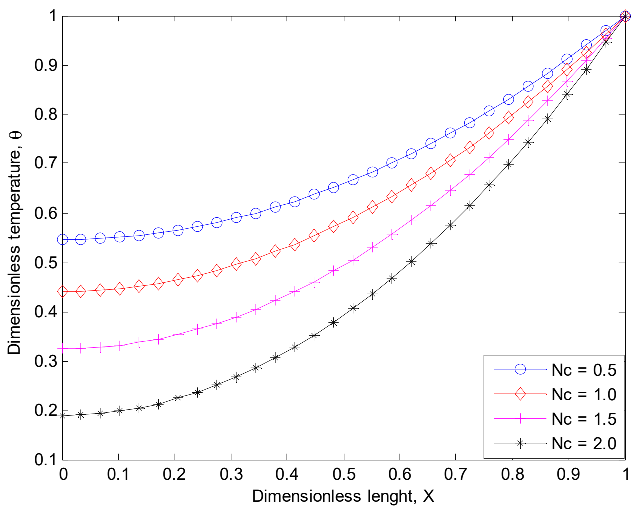

Fig. 6. Effects of convective parameter on the nondimensional temperature distribution in the fin

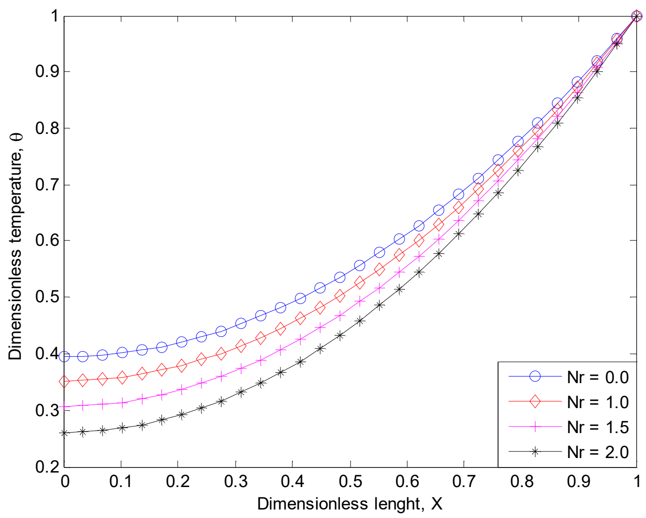

Fig. 7. Effects of radiative parameter on the nondimensional temperature distribution in the fin

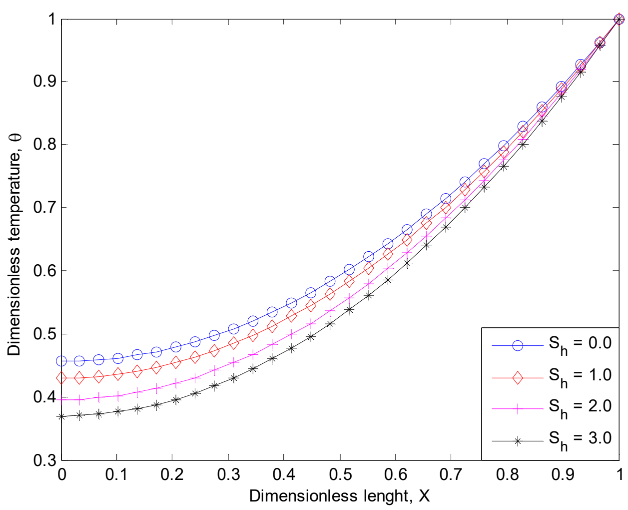

Fig. 8. Effects of porous parameter on the nondimensional temperature distribution in the fin

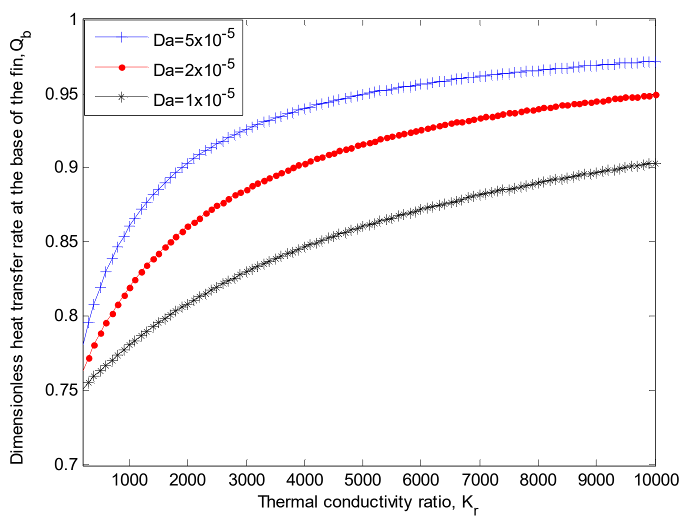

Fig. 9. Effects of Darcy number on the rate of heat transfer

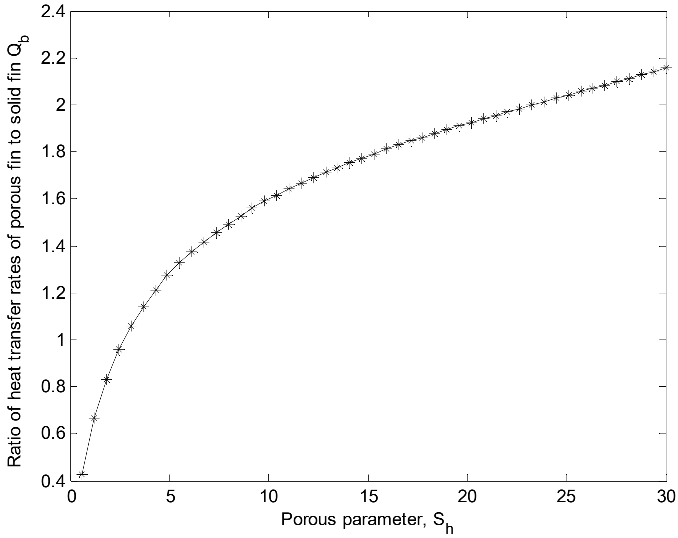

Fig. 10. Thermal performance ratio of the porous fin

Fig. 8 shows the impact of porous parameter on the dimensionless temperature distribution in the fin. The figure shows that as the porous parameter (Rayleigh number) increases the adimensional temperature in the fin decreases. The fin temperature decreases as the porosity parameter increases because of the increase in the permeability of fin which makes the working fluid to infiltrate more through the pores of the fin and increase the buoyancy force effect. Consequently, more heat is taken away from the surface of the fin as the temperature falls more. This establishes that the thermal efficiency of the fin increases as the Rayleigh number is enlarged.

The above figures show that when the convective, radiative, magnetic and porous parameters increase, the temperature drop in the fin increases which in consequent decreases thermal efficiency of the fin. Therefore, the fin is more efficient and effective for low values of convective, radiative, magnetic and porous parameters. Also, from the parametric studies, it could be clearly stated that, the fin is more efficient and effective for relatively low values of inclination of fin, convective, radiative, magnetic and porous parameters. However, these values of these parameters should be properly selected to avoid thermal stability in the fin.

The impacts of Darcy number on the heat transfer rate is shown in Fig. 9. The figure illustrates that when the Darcy number increases, the heat transfer rate from the fin increases. This is caused by the fact that because the reduction in the Darcy number causes the permeability to reduce. This in consequent causes more collision between the fluid flow and the pores of the porous. Therefore, the flowing of the fluids creates increase space to contact with the porous media which causes the fin temperature to increase.

The augmentation ratio achieved by the fin is shown in Fig. 10. The increase in the porosity parameter cause the performance ratio to increase. This is because the increased porosity parameter augments the permeability of the porous fin and increases the effects of buoyancy force. This causes more driving force for natural convection as it allows more fluid to infiltrate through the pores of the porous domain. Consequently, the rate of heat transfer rate and the performance ratio increases as it depicted in the figure.

5. Conclusion

The thermal performance of porous fin under the impacts of inclination and magnetic field has been studied in this work using finite difference method. Also, the effects of other parameters on the heat transfer model of the extended surface are investigated. The results show that increase in the fin angle of inclination and magnetic field parameter are amplified, the fin temperature decreases. Also, it was found that when the convective, radiative, magnetic and porous parameters increase, the fin temperature decreases. The results established that low values of inclination of fin, convective, radiative, magnetic and porous parameters favour thermal performance or efficiency of the fin. Therefore, the inclined porous fin is more efficient and effective for relatively low values of fin inclination, convective, radiative, magnetic and porous parameters. However, these values should be properly selected to avoid thermal stability in the fin. The present work will help in the selection of proper material for the fin and in the design of passive heat enhancement for thermal and electronic systems.

Nomenclature

A	cross sectional area
A_b	porous fin base area
c_p	specific heat capacity of the fluid passing through porous fin
h	heat transfer coefficient
k_{eff}	effective thermal conductivity
L	fin length
Ra	Rayleigh number
Rd	Radiation number
t	fin thickness of the fin
T_b	temperature at the fin base
T	fin temperature
T_a	ambient temperature, K
u	fluid average velocity
x	axial length of the fin
X	dimensionless fin length
w	width of the fin width

Greek

θ	dimensionless temperature
ε	porosity or void ratio
υ	kinematic viscosity

Author Contributions

Not applicable.

Acknowledgments

The author would like to acknowledge the materials supports and enabling environment provided by the university of Lagos, Nigeria.

Conflict of Interest

The author declared no potential conflicts of interest with respect to the research, authorship, and publication of this article.

Funding

The author received no financial support for the research, authorship, and publication of this article.

Data Availability Statements

The datasets generated and/or analyzed during the current study are available from the corresponding author on reasonable request.

References

[1] Kiwan, S., Al-Nimr, M. A., Using Porous Fins for Heat Transfer Enhancement, *Journal of Heat Transfer*, 123, 2000, 790-795.
[2] Gong, L., Li, Y., Bai, Z., Xu, M., Thermal performance of micro-channel heat sink with metallic porous/solid compound fin design, *Applied Thermal Engineering*, 137, 2018, 288-295.
[3] Ali, H. M., Ashraf, M. J., Giovannelli, A., Irfan, M., Irshad, T. B., Hamid, H. M. et al., Thermal management of electronics: An experimental analysis of triangular, rectangular and circular pin-fin heat sinks for various PCMs, *International Journal of Heat and Mass Transfer*, 123, 2018, 272-284.
[4] Saedodin, M. O. S., Olank, M., Temperature distribution in porous fins in natural convection condition, *Journal of American Science*, 7, 2011, 476.
[5] Oguntala, G. A., Abd-Alhameed, R. A., Sobamowo, M. G., Eya, N. Effects of particles deposition on thermal performance of a convective-radiative heat sink porous fin of an electronic component, *Thermal Science and Engineering Progress*, 6, 2018, 177-185.
[6] Sobamowo, M. G., Kamiyo, O. M., Adeleye, O. A., Thermal performance analysis of a natural convection porous fin with temperature-dependent thermal conductivity and internal heat generation, *Thermal Science and Engineering Progress*, 1, 2017, 39-52.
[7] Mosayebidorcheh, S., Farzinpoor, M., Ganji, D. D., Transient thermal analysis of longitudinal fins with internal heat generation considering temperature-dependent properties and different fin profiles, *Energy Conversion and Management*, 86, 2014, 365-370.
[8] Kim, S. M., Mudawar, I., Analytical heat diffusion models for different micro-channel heat sink cross-sectional geometries, *International Journal of Heat and Mass Transfer*, 53, 2010, 4002-4016.
[9] Moradi, A., Hayat, T., Alsaedi, A., Convection-radiation thermal analysis of triangular porous fins with temperature-dependent thermal conductivity by DTM, *Energy Conversion and Management*, 77, 2014, 70-77.
[10] Oguntala, G. A., Abd-Alhameed, R. A., Sobamowo, M. G. On the effect of magnetic field on thermal performance of convective-radiative fin with temperature-dependent thermal conductivity, *Karbala International Journal of Modern Science*, 4, 2018, 1-11.
[11] Wan, Z. M., Guo, G. Q., Su, K. L., Tu, Z. K., Liu, W., Experimental analysis of flow and heat transfer in a miniature porous heat sink for high heat flux application, *International Journal of Heat and Mass Transfer*, 55, 2012, 4437-4441.
[12] Naphon, P., Klangchart, S., Wongwises, S., Numerical investigation on the heat transfer and flow in the mini-fin heat sink for CPU, *International Communications in Heat and Mass Transfer*, 36, 2009, 834-840.
[13] Oguntala, G. A., Abd-Alhameed, R. A., Sobamowo, M. G., Danjuma, I., Performance, Thermal Stability and Optimum Design Analyses of Rectangular Fin with Temperature-Dependent Thermal Properties and Internal Heat Generation, *Journal of Computational Applied Mechanics*, 49, 2018, 37-43.
[14] Sobamowo, M. G., Thermal analysis of longitudinal fin with temperature-dependent properties and internal heat generation using Galerkin's method of weighted residual, *Applied Thermal Engineering*, 99, 2016, 1316-1330.
[15] Seyf, H. R., Feizbakhshi, M., Computational analysis of nanofluid effects on convective heat transfer enhancement of micro-pin-fin heat sinks, *International Journal of Thermal Sciences*, 58, 2012, 168-179.
[16] Fazeli, S. A., Hashemi, S. M. H., Zirakzadeh, H., Ashjaee, M., Experimental and numerical investigation of heat transfer in a miniature heat sink utilizing silica nanofluid, *Superlattices and Microstructures*, 51, 2012, 247-264.
[17] Oguntala, G. A., Sobamowo, G. M., Yinusa, A. A., Abd-Alhameed, R., Application of Approximate Analytical Technique Using the Homotopy Perturbation Method to Study the Inclination Effect on the Thermal Behavior of Porous Fin Heat Sink, *Mathematical and Computational Applications*, 23, 2018, 62.
[18] Oguntala, G. A., Abd-Alhameed, R. A., Haar Wavelet Collocation Method for Thermal Analysis of Porous Fin with Temperature-dependent Thermal Conductivity and Internal Heat Generation, *Journal of Applied and Computational Mechanics*, 3, 2017, 185-191.
[19] Sobamowo, M. G., Alaribe, K. C., Adeleye, O. A., Yinusa, A. A., Adedibu, O. A., A Study on the Impact of Lorentz Force on the Thermal Behaviour of a Convective-Radiative Porous Fin using Differential Transformation Method, *International Journal of Mechanical Dynamics & Analysis,* 6(+1), 2020, 45-59.
[20] Gireesha. B. J., Sowmya, G., Heat Transfer Analysis of an Inclined Porous Fin using Differential Transform Method Journal, *International Journal of Ambient Energy*, 2020, Article in Press.
[21] Jasim, H. H., Söylemez, M. S., The Effects of the Perforation Shapes, Sizes, Numbers and Inclination Angles on The Thermal Performance of a Perforated Pin Fin, *Turkish Journal of Science & Technology*, 13(2), 2018, 1-13.
[22] Jasim, H. H., Söylemez, M. S., Optimization of a rectangular pin fin using rectangular perforations with different inclination angles, 35(4), 2017, 969-977.
[23] Oguntala, G. A., Sobamowo, G. M., Abd-Alhameed, R., Noras, J., Numerical Investigation of Inclination on the Thermal Performance of Porous Fin Heatsink using Pseudospectral Collocation Method, *Karbala International Journal of Modern Science*, 5(1), 2009, 19-26.
[24] Amirkolaei, S. R., Ganji, D. D., Salarian, H., Determination of temperature distribution for porous fin which is exposed to Uniform Magnetic Field to a vertical isothermal surface by Homotopy Analysis Method and Collocation Method, *Indian J. Sci. Res.*, 1(2), 2014, 215-222.
[25] Sheikholeslami, M., Jafaryar, M., Shafee, A., Babazadeh, H., Acceleration of discharge process of clean energy storage unit with insertion of porous foam considering nanoparticle enhanced paraffin, *Journal of Cleaner Production*, 261(10), 2020, 121206.
[26] Sheikholeslamia, M., Farshad, S. A., Shafee, A., Babazadeh, H., Performance of solar collector with turbulator involving nanomaterial turbulent regime, *Renewable Energy*, 163, 2021, 1222-1237
[27] Sheikholeslami, M., Jafaryar, M., Said, Z., Alsabery, A. I., Babazadeh, H., Shafee, A., Modification for helical turbulator to augment heat transfer behavior of nanomaterial via numerical approach, *Applied Thermal Engineering*, 182(5), 2021, 115935.
[28] van Erp, R., Soleimanzadeh, R., Nela, L. *et al.*, Co-designing electronics with microfluidics for more sustainable cooling, *Nature*, 585, 2020, 211–216.
[29] Varnava, C., Chips cool off with integrated microfluidics, *Nature Electronics*, 3, 2020, 583.

ORCID iD

Gbeminiyi M. Sobamowo https://orcid.org/0000-0003-2402-1423

How to cite this article: Sobamowo G.M. Combined Impacts of Fin Surface Inclination and Magnetohydrodynamics on the Thermal Performance of a Convective-Radiative Porous Fin, *J. Appl. Comput. Mech.*, 8(3), 2022, 940–948. https://doi.org/10.22055/JACM.2020.35060.2550